

## Use of microscale coplanar striplines with indium tin oxide windows in optical ferromagnetic resonance measurements

P. S. Keatley, V. V. Kruglyak, A. Barman, S. Ladak, and R. J. Hicken<sup>a)</sup>  
*School of Physics, University of Exeter, Stocker Road, Exeter, EX4 4QL United Kingdom*

J. Scott and M. Rahman  
*Department of Physics and Astronomy, University of Glasgow, Glasgow, G12 8QQ United Kingdom*

(Presented on 8 November 2004; published online 17 May 2005)

It is shown that a coplanar stripline structure containing indium tin oxide windows can be used to perform optical ferromagnetic resonance measurements on a sample grown on an opaque substrate, using a pulsed magnetic field of any desired orientation. The technique is demonstrated by applying it to a thin film of permalloy grown on a Si substrate. The measured precession frequency was found to be in good agreement with macrospin simulations. The phase of the oscillatory Kerr response was observed to vary as the probe spot was scanned across the coplanar stripline structure, confirming that the orientation of the pulsed field varied from parallel to perpendicular relative to the plane of the sample. © 2005 American Institute of Physics. [DOI: 10.1063/1.1849071]

Ultrafast magnetization dynamics have recently attracted increasing interest due to the potential for applications in data storage technology,<sup>1</sup> while resonant mode spectra may be used to characterize the magnetic parameters of thin films.<sup>2</sup> Techniques such as optical ferromagnetic resonance (FMR)<sup>3-5</sup> and pulsed inductive microwave magnetometry<sup>6</sup> have been developed to study the magnetization dynamics of thin films and micrometer scale magnetic elements. A microscale coplanar stripline (CPS) or waveguide structure is used to deliver a pulsed magnetic field to the sample. In optical FMR the local magnetization dynamics are sensed with a delayed optical probe pulse via the magneto-optical Kerr effect (MOKE). In order to experience a significant pulsed magnetic field, the sample must be brought into close contact with the CPS, which can be achieved by depositing the sample directly onto the CPS. However, this is only feasible if the sample growth is insensitive to the substrate conditions. Wider application of the technique requires that measurements be made on samples deposited on arbitrary substrates. In Ref. 7, optical FMR measurements were made on spin valve structures fabricated on opaque substrates using a CPS fabricated on a transparent substrate. Because of the restricted optical access, measurements could only be made between the tracks of the CPS, i.e., with an out-of-plane pulsed magnetic field. However, measurements with an in-plane pulsed field are advantageous in some cases because of the stronger response of the sample, and are essential if precessional switching is to be observed.<sup>8,9</sup> Here we introduce a hybrid Au/indium tin oxide (ITO, In<sub>2</sub>O<sub>3</sub>/SnO<sub>2</sub>) CPS fabricated on a transparent substrate, which allows optical FMR measurements to be performed on magnetic samples grown on arbitrary substrates with both out-of-plane and in-plane pulsed magnetic fields. The use of the hybrid CPS is demonstrated in the magnetic characterization of a 25 nm thick permalloy film grown upon a Si substrate. The response of this simple sample is also used to characterize the spatial

profile of the pulsed magnetic field above the plane of the CPS.

The permalloy sample was deposited onto a thermally oxidized Si[100]/SiO<sub>2</sub>(100 nm) wafer by dc magnetron sputtering from a base pressure of  $5 \times 10^{-7}$  Torr. A protective 20 nm thick layer of Al<sub>2</sub>O<sub>3</sub> was deposited by rf sputtering. A bias magnetic field of 150 Oe was applied during the growth to induce a uniaxial magnetic anisotropy. For a preliminary characterization of the sample, static longitudinal MOKE loops were acquired using a cw HeNe laser. It was found that the permalloy possessed a uniaxial anisotropy field of 6 Oe.

The hybrid Au/ITO CPS was fabricated from a quartz plate precoated with a thin film of ITO (150 nm) of ~95% transparency and measured sheet resistance of ~30 Ω/square. Photoresist was spun onto the plate and patterned so as to form an etch mask with a track width and separation of 30 μm. The unwanted ITO was removed by dry etching in a methane/hydrogen plasma for 13 min at a pressure of 11 mTorr. After removal of the remaining resist, a layer of fresh resist was spun onto the plate. The new resist was exposed and developed so as to leave the full length of the CPS structure exposed apart from a 30 μm square region half way along each track. A Ti(30 nm)/Au(150 nm) bilayer was next deposited and the remaining resist lifted off. Each track was 3 mm long with a dc resistance of about 70 Ω and had a Au-free window of 30 μm width at its center. The characteristic impedance was expected to be about 200 Ω.<sup>10</sup>

The CPS structure was placed face down onto the sample, and the pump-probe measurements were performed in the time-resolved scanning Kerr effect configuration<sup>11</sup> at a wavelength of 790 nm. An optically gated current pulse generated a pulsed magnetic field around the tracks of the CPS structure, after which it was absorbed in two 47 Ω surface mount resistors placed at the end of the tracks. The temporal current profile had a complicated shape due to multiple reflections of the pulse from impedance mismatches within the transmission line and connecting circuitry. In order to avoid

<sup>a)</sup>Electronic mail: r.j.hicken@exeter.ac.uk

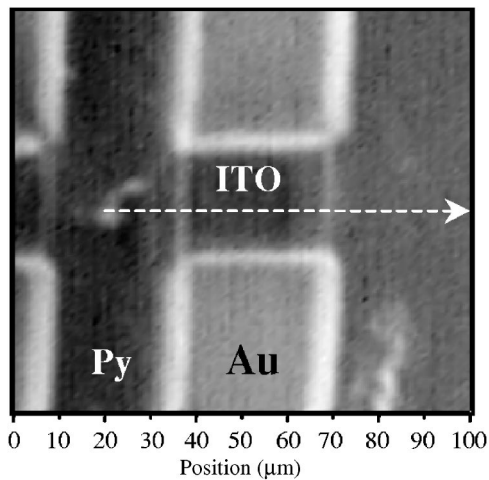


FIG. 1. Intensity image of a hybrid Au/ITO CPS track.

overlap of the current pulse with weaker delayed reflections from the preceding pulse, a commercially available pulse-picker was used to block four out of five laser pulses. The probe beam was expanded by a factor of 10, and a microscope objective of numerical aperture of 0.25 was used to focus the probe through the CPS substrate (and ITO windows) to a spot of about  $3 \mu\text{m}$  diameter on the sample surface. A scanning translation stage was used to position the spot at different positions upon the surface of the sample. The out-of-plane component of the magnetization  $M_z$  was probed by means of the polar Kerr effect, using a polarizing bridge detector. The measured Kerr signal was typically about  $0.1\text{--}0.5 \text{ m deg}$ . An in-plane bias magnetic field  $\mathbf{H}$  of variable amplitude was applied parallel to the tracks during the measurements.

Figure 1 shows an intensity image of an ITO window obtained by scanning the sample beneath the focused laser beam. The ITO window sections could be clearly seen for both tracks. Figure 2(a) shows typical time-resolved MOKE signals obtained from the regions of the sample that were subject to an in-plane pulsed field, by probing through the ITO window. Figure 2(b) shows the fast Fourier transform power spectra calculated from the time-resolved signals. The mode frequencies were extracted by fitting the spectra to a

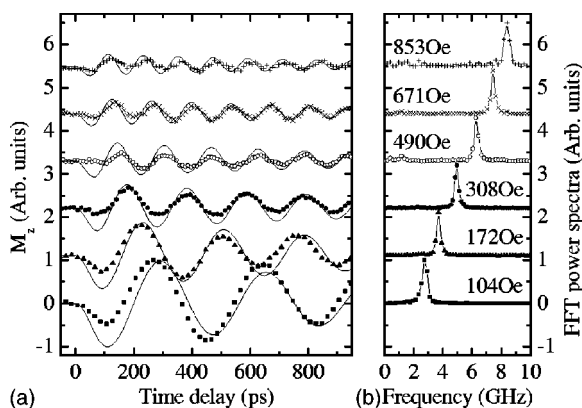


FIG. 2. (a) Typical time-resolved Kerr signals (symbols) and corresponding simulations (line) obtained by probing through the ITO window for six different bias fields. A linear background has been subtracted from the signals. (b) Fast Fourier transforms for the experimental signals in (a).

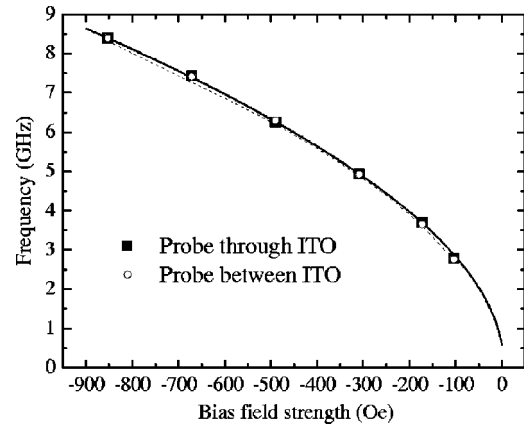


FIG. 3. Dependence of frequency on the bias field strength for time-resolved signals obtained by probing through the ITO window (filled squares) and between the ITO sections of the CPS (open circles).

Lorentzian function, and are plotted in Fig. 3 as a function of the bias field strength. The figure also shows the mode frequencies calculated in a similar manner from time-resolved signals measured between the tracks of the CPS structure where the pulsed field lies perpendicular to the plane. In each case the pulsed field was perpendicular to the bias field, and so was not expected to affect the frequency of the uniform mode precession. The frequencies measured in these two configurations are seen to agree very well.

Although the signals appear similar in the frequency domain they differ in the time domain. Figure 4 shows time-resolved MOKE signals obtained at  $5 \mu\text{m}$  intervals across the CPS structure, as shown by the white arrow in Fig. 1. Between the ITO sections of the tracks the pulsed field lies out-of-plane, whereas above the ITO window the pulsed field lies in the plane. Outside the tracks the pulsed field cants out-of-plane in the opposite direction to that between the tracks. Between these three configurations there is a gradual variation of the field orientation. The change of pulsed field orientation results in a variation of the initial torque exerted on the sample across the CPS. This leads to a variation in the phase of the time-resolved signals measured at different positions. The phase shift is illustrated in Fig. 4 by the dashed

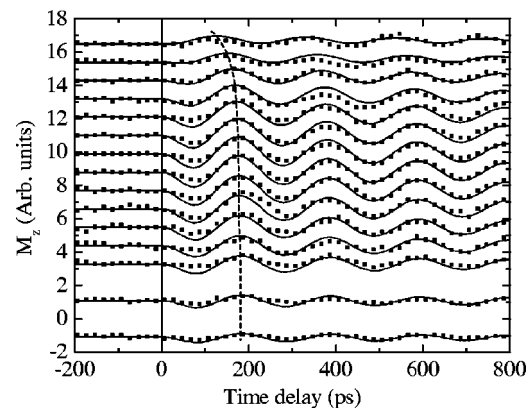


FIG. 4. Time-resolved Kerr signals measured at various positions across the CPS track (symbols) with corresponding simulations (solid lines). The signals from top to bottom correspond to positions at  $5 \mu\text{m}$  intervals along the arrow shown in Fig. 1. The dashed line illustrates the change in the phase between the different signals.

line drawn through the first positive peak of each signal.

In order to confirm our interpretation of the experimental results, we performed macrospin simulations of the magnetization dynamics of the sample at different positions under the CPS. We solved the Landau–Lifshitz equation<sup>12</sup> in the small angle approximation<sup>6</sup> to obtain the following expression for the mode frequency  $\omega$ :

$$\omega^2 = \gamma^2 \left[ H \cos \phi + \frac{2K_u}{M} \cos[2(\phi - \phi_K)] \right] \times \left[ H \cos \phi + \frac{2K_u}{M} \cos^2(\phi - \phi_K) + 4\pi M \right], \quad (1)$$

where  $\gamma$ ,  $K_u$ , and  $M$  are the gyromagnetic ratio, anisotropy constant, and magnetization, respectively.  $\phi$  and  $\phi_K$  are the angles subtended by the static magnetization and uniaxial anisotropy axis with the applied field. The dependence of the frequency upon the bias field strength was first fitted to Eq. (1) in the quasialignment approximation, i.e., assuming that the static magnetization of the sample lies parallel to the bias field. The fitted curve is shown by the solid line in Fig. 3. Assuming a value of 2 for the  $g$  factor and using the measured value of the anisotropy field, a value of  $770 \text{ emu/cm}^3$  was extracted for the magnetization, which lies close to the bulk value for permalloy. The dashed line shows a macrospin simulation of the field dependence of the frequency in which the static orientation of the sample magnetization was calculated using the steepest descent method. The curves are in good agreement, justifying the assumption made in the fitting. The extracted magnetic parameters were used to simulate the shape of the time-resolved signals for different values of the bias magnetic field and for different positions of the probe spot on the sample surface, as shown in Figs. 2(a) and 4, respectively.

The simulated dynamics of  $M_z$  shown by the curves in Fig. 2(a) reproduce the reduction of frequency and the increased amplitude of the uniform mode as the applied field strength is decreased. The pulsed field was assumed to rise to its peak value after 60 ps and the in-plane and out-of-plane components of the pulsed field were calculated by the integration of the Biot–Savart law over two strips of uniform current density with dimensions equal to those of the CPS tracks. In order to estimate the peak value of the current pulse propagating along the CPS tracks, the voltage drop across one of the surface mount resistors was measured with a 500 MHz bandwidth oscilloscope. To account for the finite bandwidth of the instrument, the decay of the pulse profile was fitted to an exponential function, yielding a relaxation time of 5.1 ns. The peak voltage was taken to be the value of this exponential function at the time at which the measured signal initially rose to 50% of its maximum value. This method yielded an estimated peak current value of 31.4 mA. The magnetic field was calculated for heights above the CPS, in the range of 0.5 to  $50 \mu\text{m}$ . The best agreement between the phase and amplitude of the measured and simulated signals at different positions across the CPS structure was obtained for an assumed separation of  $30 \mu\text{m}$  between the sample and CPS. At this separation the magnitude of the in-plane and out-of-plane pulsed field at the sample position

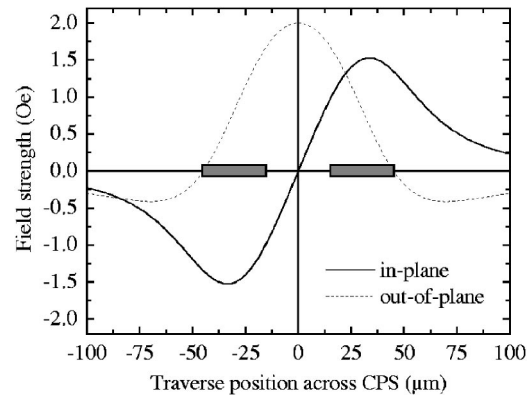


FIG. 5. Spatial profile across the CPS for the in-plane and out-of-plane components of the pulsed magnetic field calculated for a track-sample separation of  $30 \mu\text{m}$ .

was estimated to be 1.5 and 2.0 Oe, respectively. The good agreement between experiment and simulation confirmed that the orientation of the pulsed field varied between parallel and perpendicular to the plane of the sample, as shown in Fig. 5. Since the orientation of the pulsed field varies across the CPS track the initial torque on the sample magnetization will vary. This causes the magnetization to be deflected in different directions at different positions across the track. Therefore, the measured  $M_z$  will appear delayed when the magnetization initially moves in-plane prior to canting out-of-plane.

In summary we have demonstrated that a hybrid Au/ITO CPS allows magnetization dynamics to be studied in a sample fabricated on an opaque substrate, following excitation by either an in-plane or an out-of-plane pulsed magnetic field. We have shown that a phase shift exists in the time-resolved MOKE signals obtained at different positions across the ITO window. Macrospin simulations confirm the variation of the pulsed field between the out-of-plane and in-plane configurations.

The authors gratefully acknowledge the provision of financial support by the U. K. Engineering and Physical Sciences Research Council and by the Wohlfarth Memorial Fund of the Magnetism Group of the Institute of Physics.

- <sup>1</sup>W. K. Hiebert, A. Stankiewicz, and M. R. Freeman, *Phys. Rev. Lett.* **79**, 1134 (1997).
- <sup>2</sup>R. E. Camley, *J. Magn. Magn. Mater.* **200**, 583 (1999).
- <sup>3</sup>A. Barman, V. V. Kruglyak, R. J. Hicken, J. M. Rowe, A. Kundrotaitė, J. Scott, and M. Rahman, *Phys. Rev. B* **69**, 174426 (2004).
- <sup>4</sup>M. Belov, Z. Liu, R. D. Sydora, and M. R. Freeman, *Phys. Rev. B* **69**, 094414 (2004).
- <sup>5</sup>B. C. Choi, G. E. Ballentine, M. Belov, and M. R. Freeman, *Phys. Rev. B* **64**, 144418 (2001).
- <sup>6</sup>T. J. Silva, C. S. Lee, T. M. Crawford, and C. T. Rogers, *J. Appl. Phys.* **85**, 7849 (1999).
- <sup>7</sup>A. Barman, V. V. Kruglyak, R. J. Hicken, C. H. Marrows, M. Ali, A. T. Hindmarch, and B. J. Hickey, *Appl. Phys. Lett.* **81**, 1468 (2002).
- <sup>8</sup>W. K. Hiebert, G. E. Ballentine, and M. R. Freeman, *Phys. Rev. B* **65**, 140404 (2002).
- <sup>9</sup>Th. Gerrits, H. A. M. van den Berg, J. Hohlfield, L. Bar and Th. Rasing, *Nature (London)* **418**, 509 (2002).
- <sup>10</sup>K. C. Gupta, R. Garg, and I. J. Bahl, *Microstrip Lines and Slotlines* (Artech House, Boston, 1979), p. 266.
- <sup>11</sup>R. J. Hicken, *Philos. Trans. R. Soc. London, Ser. A* **361**, 2827 (2003).
- <sup>12</sup>L. Landau and E. Lifshitz, *Phys. Z. Sowjetunion* **8**, 153 (1935).